

## Original Article



# A DTF and Molecular thermodynamic Simulation on the Adsorption Inhibition of Cytarabine a Nucleotides as a Potential Inhibitor on the Alumnium Metal Surface

Fater Iorhuna<sup>1,\*</sup> , Abdullahi Muhammad Ayuba<sup>1</sup> , Thomas Aondofa Nyijime<sup>2</sup> , Hussein Muhammedjamiu<sup>1</sup>

<sup>1</sup>Bayero University, Department of Pure and Industrial Chemistry, Kano, 700241, Nigeria

<sup>2</sup>Department of Chemistry, Joseph Saawuan Tarka University, Makurdi, Benue, Nigeria



**Citation** F. Iorhuna, A. M. Ayuba, N. A. Thomas, H. Muhammedjamiu, **A DTF and Molecular thermodynamic Simulation on the Adsorption Inhibition of Cytarabine a Nucleotides as a Potential Inhibitor on the Alumnium Metal surface.** *Eurasian J. Sci. Technol.*, 2023, 3(4), 211-222.

<https://doi.org/10.48309/EJST.2023.410063.1084>

**Article info:**

**Received:** 2023-08-05

**Revise:** 2023-09-06

**Accepted:** 2023-10-13

**ID:** EJST-2308-1084

**Checked for Plagiarism:** Yes

**Checked Language:** Yes

**Keywords:**

Aluminum, Cytarabine, Fukui-function, Physiosorption, Simulation.

**ABSTRACT**

In this study, the substance was theoretically examined using computational techniques to provide more analysis on the cytarabine inhibition on the aluminum surface. Through DFT and molecular dynamic simulations, the quantum chemical approach was used to study the parameters. Al (110) surface was chosen because of the atoms' close proximity and density on the surface. The local and global reactivity, as well as the Fukui function, were computed to determine the molecule's reactivity. The mechanism of cytarabine is assumed to display physiosorption with aluminum surface based on the predicted adsorption and binding energies (-52.476 and 52.476 Kcal/mol) and the negative value of the EHOMO which is -5.133eV. In conclusion, the molecule is described as an efficient aluminum inhibitor having just a mild inhibition on the studied aluminium surface.

**Introduction**

**W**ith the sense of reality, corrosion can be only reduced significantly or delayed to a reasonable extent. Corrosion is an ugly phenomenon that is disturbing the engineering aspect of the construction work in the world today [1-3]. It is defined as the washing away of the metal surface with -some harsh environmental conditions like high

temperature, pressure, and high concentration of acids like HCl and H<sub>2</sub>SO<sub>4</sub> [4].

In oil sectors of the economy, HCl is used as a pickling agent for the cleaning of the oil tanks which in turn bring about the washing away of the tank involved [5-6]. The use of mechanical inhibitors such as coating the surface with other metals was approached by early scientist by galvanizing the surface of interested metals.

\*Corresponding Author: Fater. Iorhuna. [uverter22@gmail.com](mailto:uverter22@gmail.com)

Today, the attention has been shifted to the green environment providing enough biodegradable materials with the addition of small quantity of chemicals called inhibitors; this forms a film layer on the metal surface by stopping or slowing down the rate of metal decomposition around the metallic environment [7].

According to separate studies by Ayuba and Umar, the presence of unpaired electrons or unstable bonds ( $\pi$ -bonds) between methylene (-CH<sub>2</sub>-) and some heteroatoms, including nitrogen, sulphur, and oxygen among others, has a convincing inhibiting effect on the metals surface. Quantum chemistry theories were utilized through computer analysis to its accomplishment [7-8].

Calculations based on quantum chemistry are used to determine how inhibitor compounds interact with metal surfaces. The application of theoretical parameters enables the description of inhibitor molecule structures and offers a theory for how they interact with metal surfaces [9-12].

A good approach to determine the actual interaction and adsorption energy between the inhibitor molecule and metal surfaces is molecular dynamic modeling [7].

These compounds are either in inorganic, organic, or condensed matter, according to theoretical studies utilizing computational methods recently done to predict their electronic, structural, and molecular features in compounds that have been demonstrated to be potential corrosion inhibitors [13-14].

It was discovered that the chemical and electronic characteristics of inhibitor molecules were substantially connected with the efficacy of their inhibition [15]. The use of time- and money-consuming conventional methods to reduce corrosion, such as the weight loss method, potentiodynamic polarization, and electrochemical impedance spectroscopy, is not advised for this drill. Instead, theoretical approaches that address these shortcomings are strongly advised [1-6].

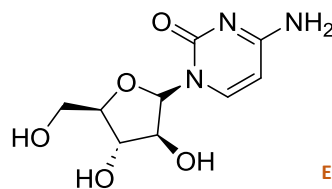
In this work, theoretical (DFT) and simulation methods were used to examine the corrosion inhibition potential of the nucleotide cytarabine (CTB), which is 4-Amino-1-(3,4-dihydroxy-5-hydroxymethyl-tetrahydrofuran-2-yl)-1H-

pyrimidin-2-one. The molecule was selected based on the presence of glycosides with the idea that since glycosylated compounds served as a validated platform for the development of many current front-line drugs, they may also have potential in treating some of the metals we have purified over the years. Since the aluminum crystal surface was selected, it is thought to have more surface coverage than alternatives like Al (111), etc.

Using molecular dynamic simulation, the goal is to ascertain the molecule mode of adsorption on the aluminum surface, the adsorptive capacity, and the active sites.

Energy of the highest occupied molecular orbital (EHOMO), energy of the lowest unoccupied molecular orbital (ELUMO), energy gap (E), total energy (E), electron affinity (A), ionization potential (I), global hardness ( $\eta$ ), global softness (S), Second Fukui function, and Fukui functions  $f(r)$ , at the geometry optimizing level, are some of the properties taken into consideration.

To operate with a reasonable temperature that will not be too high or too low for the inhibition process on the simulated surface, the temperature was chosen.



Eurasian Journal of  
Science and Technology

Figure 1 cytarabine (CTB)

## Computational Methods

### Sketching and Geometric Optimization of the Molecules

CambridgeSoftware Chem Draw Ultra 7.0.3 was used to create a drawing of the substance under examination. Utilizing the DNP+

foundation and DMol<sub>3</sub>, the molecule was improved for DFT-D limited spin polarization. B3LYP was chosen for the water solvent's local density functional [1-7]. According to Koopman's theory, Equations (2) and (3), respectively, relate the energy of the border molecular orbital, the energy of the highest occupied molecular orbital (EHOMO), and the energy of the lowest unoccupied molecular orbital (ELUMO) [14-17].

$$\text{Ionization energy (IE)} = -EHOMO \quad (1)$$

$$\text{Electron Affinity (EA)} = -ELUMO \quad (2)$$

According to Pearson, the value of global hardness ( $\eta$ ) may be roughly approximated by Equation (3). Equation (4) demonstrates that the global softness (S) of the system is the opposite of the global hardness. Equations (5) and (6) are used to derive the global electrophilicity index and nucleophilicity, respectively [7,9].

$$\text{Half Electron transfer Change } (\Delta N) = \frac{\chi^{Fe} - \chi^{Inh.}}{2(\eta^{Fe} + \eta^{Inh.})} \quad (8)$$

$$\text{Energy of Back donation Effect } (\Delta E_{bd}) = \frac{-\eta}{4} \quad (9)$$

$$\text{Absolute electronegativity (eV) } (\chi) = \chi = \frac{I+A}{2} = \frac{-1}{2}(E_{HOMO} - E_{LUMO}) \quad (10)$$

The second order Fukui function ( $f_2$ ) and the dual descriptor  $f(k)$  were used to describe the donating and acceptability of the molecule and

$$\text{Fukui Function (+)} f(k)^+: \text{ (for nucleophilic attack)} = qk(N+1) - qk(N) \quad (11)$$

$$\text{Fukui Function (-)} f(k)^-: \text{ (for electrophilic attack)} = qk(N) - qk(N-1) \quad (12)$$

$$\text{Fukui function } f(r) = f(k)^+ - f(k)^- = f^2 \quad (13)$$

### Molecular Dynamics Simulation

A simulation box measuring 17 x 12 x 28 with a periodic boundary condition was used to carry out computations to mimic a realistic piece of the surface. The Al crystals along (110), and the Al crystals along the (1 1 1) Plane, were separated using the fractional depth of 3.0. The lower layers' form was constrained prior to iron surface optimization, and then the iron surface

$$\text{Global Hardness } (\eta) = \frac{IE-EA}{2} \quad (3)$$

$$\text{Global softness (S)} = \frac{1}{\eta} \quad (4)$$

$$\text{Global electrophilicity index } (\omega) = \frac{\chi^2}{2\eta} \quad (5)$$

$$\text{nucleophilicity Index } (\varepsilon) = \frac{1}{\omega} \quad (6)$$

Using the connection provided in Equation (7), the molecules' energy gap is computed. The stability of compounds on surfaces is controlled by this parameter called the energy gap.

$$\text{Energy Gap } (\Delta Eg) = ELUMO - EHOMO \quad (7)$$

Equation (8) is used to compute the percentage of electrons that pass from the inhibitor to the Al-surface (N). A metric that shows the rate of electron transfer on the surface is the molecules' half electron transfer.

While back-donation is calculated, as shown in Equation (9).

the metal, which has a theoretical electronegativity value (Al=5.6eV) and a global hardness of 0eV [2-5].

was expanded into a 10 x 10 supercell [1-4] to reduce edge effects. A trade-off was made between a system with too much kinetic energy, where the molecule desorbs from the surface, and a system with not enough kinetic energy, where the molecule is unable to move across the surface, by lowering the temperature to 350 K to quench the molecules on the surface. [1-2,21].

The temperature was set using the NVE (microcanonical) ensemble with a time step of 1 fs and a simulation duration of 5 ps. The device was set up to quench every 250 steps on both

surfaces to collect statistical values for the energies on the Al surface. Forcite model and surface designs were used to create various interactions. The binding energy between the inhibitors and the metal surfaces was calculated using the connection in Equation (14) [22].

$$\text{Binding Energy} = E_{\text{total}} - (E_{\text{inhibitor}} + E_{\text{Fe surface}}) \quad (14)$$

Where,

$E_{\text{total}}$  = Total energy,  $E_{\text{inhibitor}}$  = Energy of inhibitor,  $E_{\text{Fe surface}}$  = Energy of the metal surface

## Results and Discussion

### Quantum Chemical Calculations

#### Molecular Geometry

With a B3LYP functional and DNP+ basis set in the aqueous phase; density functional theory (DFT) was employed to fully optimize the geometry of the compound cytarabine (CTB) structure. For the form of the molecule on the Al surface before and after simulation, Table 1a presents the bond link and Table 1b lists the torsion angle between the atoms. The bond length or bond distance of a molecule is the typical separation between two bonded atoms [18]. The Armstrong (A) bond length is displayed in Figures 2(a) and (b) for both the simulated and geometry-optimized molecule configurations. The bond lengths between the atoms in molecules with simulated forms have been demonstrated to vary as the structural orientation of the atoms is changed [7,9].

Any relationship must be broken with energy of a certain value. The closer atoms' nuclei are to one another, the more energy is needed to separate them because of the strong force of attraction between them [18-20]. In other words, it takes a lot of dissociation energy to break a weak link [8-9]. During geometry optimization and at the simulated molecule, the heteroatoms (nitrogen and oxygen) coupled to a carbon atom exhibit a shorter bond length than the carbon-to-carbon bond length, as seen in Figure 2a. The geometry also revealed that the hashed wedge bonds of the molecule were longer than solid single bonds. However, the stronger ties that bound the molecule's

glycoside hinted that bonds may form and break easily [18-25].

The results here demonstrated that there is a great potential for electron transfer between the metal and surface if the glycoside of the molecule is employed to stop the corrosion of metals like aluminum. Both variants of the molecule for the subject molecule are completely planar, as shown by the optimized structure's torsional angles in Figure 2b and the simulated structure values of the molecule. This suggests that molecules have a preference for flattening out when they adsorb on metal surfaces, increasing the surface coverage. Salient bond lengths in the optimized and simulated versions of the same molecule were compared [18] to show how adsorption influences the bond's strength.

#### Fukui Function

By choosing the location where the reaction is most likely to occur, whether by donating or withdrawing electrons, molecules' local reactivity increases during electron transfer [19]. A molecule's point of attack may be determined using the radical Fukui function ( $f_0$ ), electrophilic Fukui function ( $f^-$ ), and nucleophilic Fukui function ( $f^+$ ) [18]. Only the nucleophilic ( $f^+$ ) and electrophilic ( $f^-$ ) Fukui functions were examined in this study, and the results of those with the highest values are demonstrated in Figure 3a. The data suggest that interactions may occur at atoms that are attached to rings, but not to glycosides. This demonstrated that the glycoside portion of the molecule would be less effective than the ring containing nitrogenous atoms, even if it contributed to the adsorption strength of corrosion prevention. The results show that molecules with nitrogenous atoms are more effective in deterring corrosion than those with other atoms.

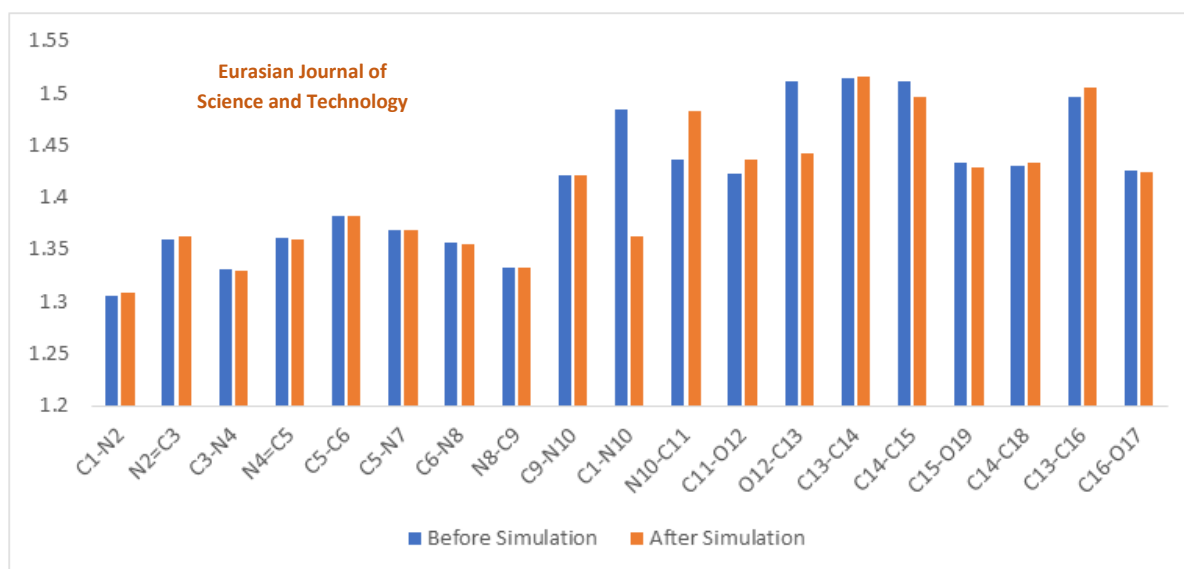


**Figure 2a** Calculated link length (Å) of the molecule CTB

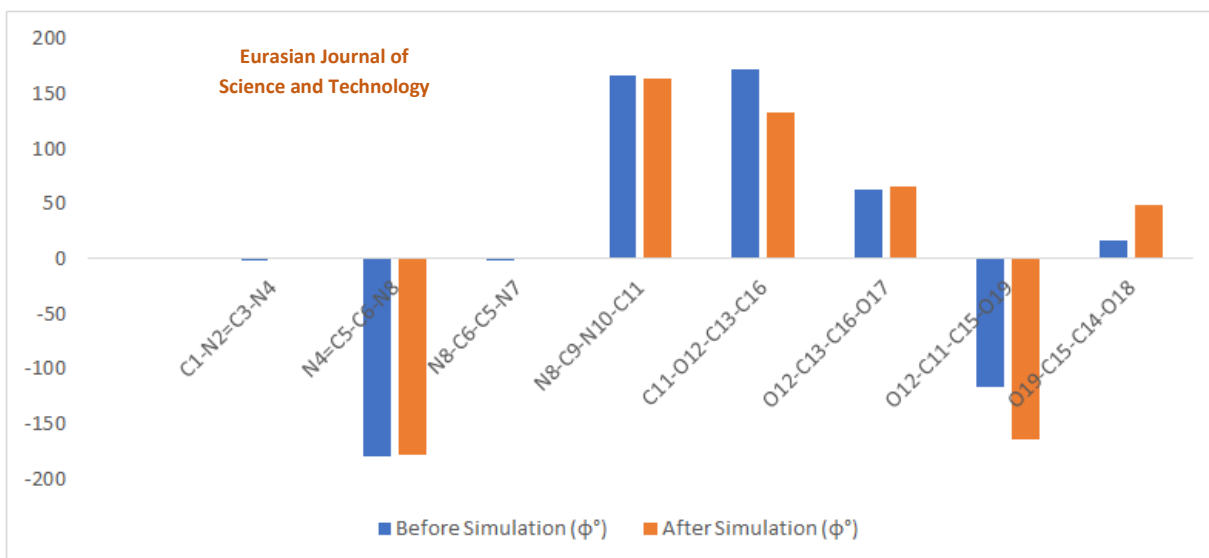


**Figure 2b** Bond angles (φ°) of the molecule CTB

As illustrated by Figure 3b, the second Fukui function result for the molecule revealed that its rates of receiving electrons from the metal surface and donating them were comparable in both negative and positive directions [26]. The ability of molecules to donate electrons to the aluminum metal's p-orbitals is supported by positive plot direction, whereas molecules that accept from the metal are supported by negative plot direction [27,28].

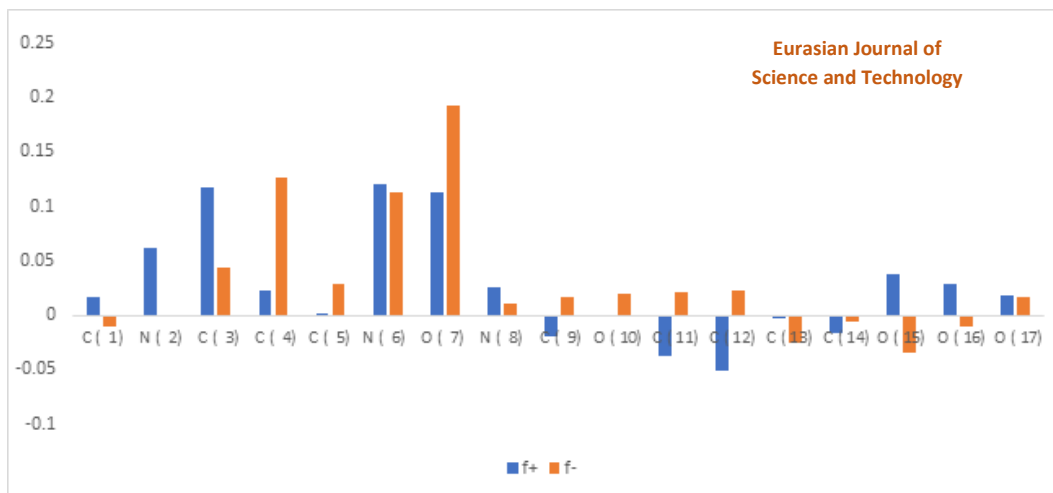


**Figure 3a** The Fukui functions of the Molecule CTB

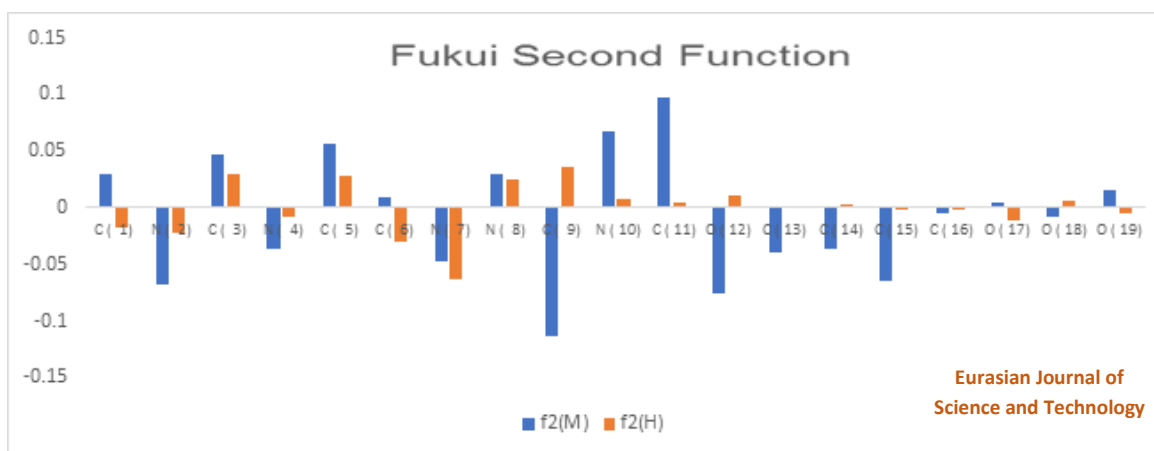


**Figure 3b** The Second Fukui function of the Molecule CTB

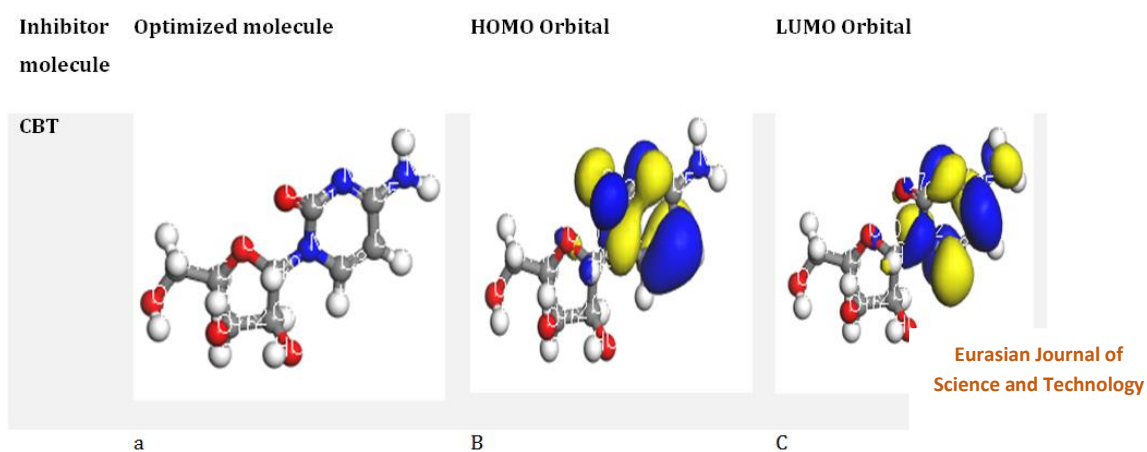


**Figure 4** (a) Optimized Geometry (b) Highest Occupied Molecular Orbital (c) Lowest Unoccupied Molecular Orbital

### Chemical Quantum Parameters

Figure 4 displays the HOMO and LUMO orbitals of the compounds under investigation as well as the CBT molecule that has been optimized. The graphic shows that the HOMO and LUMO orbitals are only widely dispersed in the ring structure that contains the nitrogen atom. The glycoside part of the molecule was not covered by the HOMO and LUMO coverage of the interaction. This proves that the glycoside was not involved in the electron transfer during the whole inhibitory action of the molecule. Quantum chemical techniques are crucial in the study of corrosion because they allow for a fast examination of the structure and behavior of corrosion inhibitors. Chemical quantum parameters include the energy gap (E), the electron affinity (E.A), the ionization potential (I.E), the global hardness ( $\eta$ ), the global softness (S), the global electrophilicity index, the nucleophilicity, the half-electron transfer (N), the electron donating power (-), the electron accepting power (+), and the back donation (Ebd) [25-28]. The energy of the frontier molecular orbitals, which are the energy of the highest occupied molecular orbital (EHOMO) and the lowest unoccupied molecular orbital (ELUMO), is mentioned to be connected to the ionization potential (IE) and the electron affinity (EA) in Koopman's theory. The bulk of other estimated variables in this study had to do with the molecule's EHOMO and ELUMO, ionization energy or activation energy [18]. To make a new bond and enhance the quantity of energy released, a molecule with a lower ELUMO value finds it simpler to collect electrons from the orbitals of a metal surface. The value of  $E_g$  (ELUMO-EHOMO), which measures the difference in orbital energies between ELUMO and EHOMO, is an essential stability indicator. Better stability and less responsiveness from higher  $E_g$  levels lead to reduced inhibition efficiency. Low values of  $E_g$  lead to increased inhibition efficiency because less excitation energy is required to remove an electron from the last occupied orbital [18-20]. The energy gap, EHOMO, and ELUMO values discovered in the study are in agreement with those

discovered in separate investigations by Nyijime et al. and Uwakwe *et al.* [9,18]. Nyijime and Uwakwe established the simplicity of the reaction between the surface and the molecules with such an energy gap. Good stability and chemical inertness are both indicated by low and high ionization energies, respectively [1-5]. Strong inhibitory effectiveness is seen at moderate and equal to CBT ionization energies of 5.133(eV) [30]. Absolute hardness and softness are important characteristics to evaluate a molecule's stability and reactivity. It is clear that "chemical hardness" refers to the capacity to tolerate polarization or deformation of an atom, ion, or molecule's electron cloud under circumstances where the chemical reaction is only marginally hampered [28]. Soft molecules have a small energy gap compared to rigid molecules, which have a large one [18].

Two other linked aspects of the molecule's electrical structure are its ionization potential (IP) and electron affinity (EA). The HOMO and LUMO values fall as the IP and EA values rise in the CBT structure. This demonstrates the strong electron polarizability and excellent donor properties [7]. In its most basic form, chemical hardness refers to resistance to polarization or distortion of the electron cloud of atoms, ions, or molecules in the presence of tiny chemical reaction disturbances. In contrast to the large energy gap of a hard molecule, soft molecules have a smaller energy gap. The energy gap of the molecule suggests that it is soft, according to CBT. In addition, the global softness value is less than unity in comparison to the molecule's hardness, which is greater than unity [16-17,28]. The back donation Eb-d energy parameter may be also used to confirm the contact between the inhibitor and the metal surface. If the global hardness is positive and the energy of back donation (Eb-d) value is negative, the back donation process is improved. The inhibitor molecules transmit charge to the aluminum metal when they come into contact with the surface of the iron, as shown by Table 1's positive global hardness values for the molecules. While a molecule's ability to accept electrons is indicated by the electrophilicity index ( $\omega$ ). The ability of a molecule to provide or

receive electrons is referred to as nucleophilicity ( $\epsilon$ ), which is the opposite of electrophilicity ( $1/\omega$ ). According to research, compounds with high nucleophilicity values successfully prevent corrosion when compared to molecules with high electrophilicity indices. Table 1 presents that only 0.619% of the electrons was transferred by the inhibitor molecule to the surface of the aluminum [18]. This is under the 3.6% threshold value set out by Ayuba *et al.*, who claim that an electron transfer, rather than a molecule's size, is responsible for a molecule's improved N inhibition efficacy. This suggests

that the inhibitor's ability to provide electrons to the metal surface enhanced the CBT molecule's ability to be inhibited [7,9]. According to the power of electron donor and acceptor estimated from the molecule obtained from the computation was high, indicating that the molecule has a greater capacity for electron donation and acceptance, a larger electron accepting power (+) value translates into a stronger capacity to receive charge, whereas a lower electron donating power (-) value of a system makes it a better electron donor [7].

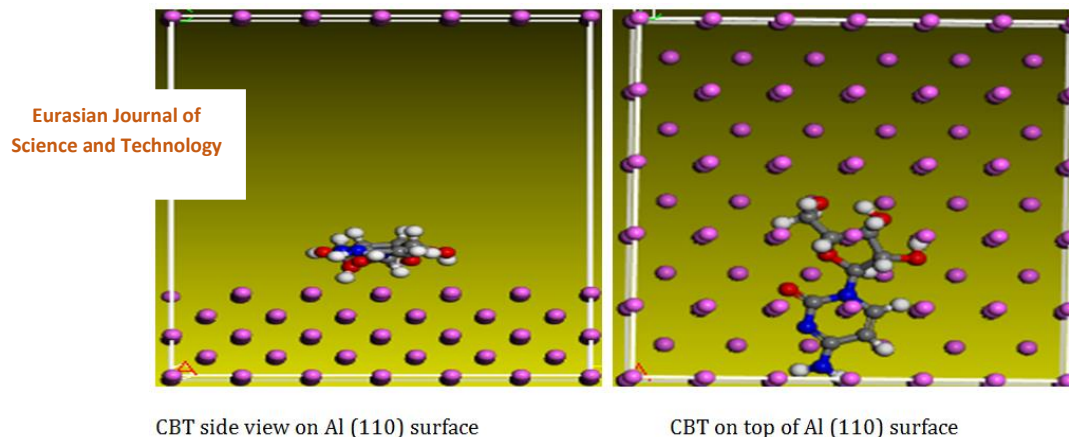
**Table 1** Quantum Chemical parameters of the molecule

| Parameters studied                      | CBT    |
|---|--------|
| $E_{HOMO}$ (eV)                         | -5.133 |
| $E_{LUMO}$ (eV)                         | -1.239 |
| I.P (eV)                                | 5.133  |
| EA (eV)                                 | 1.239  |
| $\Delta E$ (eV)                         | 3.894  |
| electronegativity( $\chi$ )             | 3.186  |
| Global hardness ( $\eta$ )              | 1.947  |
| Global softness(S)                      | 0.514  |
| Global electrophilicity index           | 2.607  |
| Nucleophilicity                         | 0.384  |
| Half-electron transfer( $\Delta N$ ) Al | 0.619  |
| ( $\omega^-$ ) Electron donating power  | 4.443  |
| ( $\omega^+$ ) Electron accepting power | 1.257  |
| ( $\Delta E_{bd}$ ) Back donation       | -0.487 |

### Dynamic Simulation of Molecules

As depicted in Figure 5, the forcite quench was used to sample a wide variety of low-energy configurations and to pinpoint the tight contacts between the inhibitor molecules CBT and Al (110) surface for adsorption at 350 K. The

system's equilibration was established by the steady average values of energy and temperature [18-19]. According to molecular dynamics modeling, Table 2 shows the calculated contact, binding, and adsorption energies between the inhibitor molecules and the aluminum surface.



CBT side view on Al (110) surface

CBT on top of Al (110) surface

**Figure 5** Showing the molecule CBT side and top view on the Al (110) crystal surface



**Table 2** Energies of the molecule After Simulation with the surfaces Al (110)

| Properties (kJ.mol <sup>-1</sup> ) CBT | Al          |
|--|-------------|
| Total Potential Energy                 | -77.221±0.1 |
| Energy of the Molecule                 | -24.694±0.1 |
| Energy of Al (110)                     | 0.000 ±0.0  |
| Adsorption energy                      | -52.476±0.1 |
| Binding energy                         | 52.476±0.1  |

### Mechanism of inhibition

The fact that the inhibitory process has a negative adsorption energy value illustrates how possible and spontaneous the interaction of molecules with metal surfaces is [9-12]. The binding energy of the molecule was 52.476 on the aluminum surface. This demonstrates that the CBT molecule's adsorption on the aluminum surface is a relatively small physical adsorption. [7]. Iorhuna *et al.* demonstrated that the starting point for chemical adsorption is 100 kcal/mol [2], further supporting the physical adsorption of the process. If the inhibitory mechanism is physical, EHOMO has a negative value [18]. The values of the adsorption energies between surfaces in the simulated reaction results of the inhibitor molecule on Al (110) surface investigated were -52.476 Kcal/mol. According to the findings of their separate studies, Belghi *et al.* and Nyijime *et al.* [9,21] and Nyijime *et al.* [4-6], respectively, physisorption characterizes this type of contact between the molecule and the metal surface during corrosion inhibition. The features reveal a little inhibition on the aluminum surface for the physically bound CBT molecule.

### Conclusion

Corrosion inhibitor CBT can be used to prevent corrosion on metallic surfaces since the interactions between a metal and the inhibitors modify their features, as investigated by specific factors. A corrosion inhibitor was researched using the Density Function Theorem (DFT). Analysis results showed that:

(1) The CBT molecules were reactive by acting as a donor, which confirms the expected inhibition, as seen by the low ELUMO and high EHOMO. The corrosion-inhibiting effectiveness of CBT molecules is significantly influenced by

the electronegativity atoms, and the electrons with a negative charge represent the potential of a HOMO center.

(2)The inhibitor molecules' heteroatoms increase the ability to adsorb on the aluminum surface by giving and absorbing electrons. The oxygen and nitrogen atoms in the inhibitor molecules as well as the coordination link between the inhibitor molecules and the aluminum p-orbitals on the halogen atoms are what make the inhibitor effective.

(3)The simulation's binding energy values show low amounts of energy, which point to slight inhibition with the surface and, given their low values, also point to physical adsorption.

### Conflict of interest

The authors declare that there is no conflict of interest in this article.

### Acknowledgements

For the BIOVIA Materials Studio software, the authors are thankful to Dr. Ayuba of Pure and Industrial Chemistry at Bayero University Kano in Kano State, Nigeria.

### ORCID

Fater Iorhuna

<https://orcid.org/0000-0002-1018-198X>

Abdullahi Muhammad Ayuba

<https://orcid.org/0000-0002-2295-8282>

Nyijime Aondofa Thomas

<https://orcid.org/0000-0001-9537-1987>

### References

- [1] AlMashhadani H.A., Saleh K.A., Electrochemical Deposition of Hydroxyapatite Co-Substituted By Sr/Mg Coating on Ti-6Al-4V

- ELI Dental Alloy Post-MAO as Anti-Corrosion, *Iraqi Journal of Science*, 2020, 2751 [[Crossref](#)], [[Google Scholar](#)], [[Publisher](#)]
- [2] Iorhuna F., Ayuba A., Nyijime A., Hussain M., Ibrahim M., Comparative Study of Halogen Substituted Isocyanatophosphine as an Adsorptive Inhibitor on Al (110) Crystal Surface, using Density Functional Theory.', *Progress in Chemical and Biochemical Research*, 2023, 6:211 [[Crossref](#)], [[Publisher](#)]
- [3] Afandiyeva L., Abbasov V., Aliyeva L., Ahmadbayova S., Azizbeyli E., El-Lateef Ahmed H.M., Investigation of organic complexes of imidazolines based on synthetic oxy-and petroleum acids as corrosion inhibitors, *Iranian Journal of Chemistry and Chemical Engineering*, 2018, 37:73 [[Crossref](#)], [[Google Scholar](#)], [[Publisher](#)]
- [4] Jafari H., Mohsenifar F., Sayin K., Effect of alkyl chain length on adsorption behavior and corrosion inhibition of imidazoline inhibitors, *Iranian Journal of Chemistry and Chemical Engineering (IJCCE)*, 2018, 37:85 [[Crossref](#)], [[Google Scholar](#)], [[Publisher](#)]
- [5] Elmi S., Foroughi M.M., Dehdab M., Shahidi-Zandi M., Computational evaluation of corrosion inhibition of four quinoline derivatives on carbon steel in aqueous phase, *Iranian Journal of Chemistry and Chemical Engineering (IJCCE)*, 2019, 38:185 [[Crossref](#)], [[Google Scholar](#)], [[Publisher](#)]
- [6] Noorollahy Bastam N., Hafizi-Atabak H.R., Atabaki F., Radvar M., Jahangiri S., Electrochemical Measurements for the Corrosion Inhibition of Mild steel in 0.5 M HCl Using poly (epichlorohydrin) Derivatives, *Iranian Journal of Chemistry and Chemical Engineering*, 2020, 39:113 [[Crossref](#)], [[Google Scholar](#)], [[Publisher](#)]
- [7] Ayuba A.M., Umar U., Modeling vitexin and isovitexin flavones as corrosion inhibitors for aluminium metal, *Karbala International Journal of Modern Science*, 2021, 7:4 [[Crossref](#)], [[Google Scholar](#)], [[Publisher](#)]
- [8] Popoola L.T., Aderibigbe T.A., Lala M.A., Mild Steel Corrosion Inhibition in Hydrochloric Acid Using Cocoa Pod Husk-Ficus exasperata: Extract Preparation Optimization and Characterization, *Iranian Journal of Chemistry and Chemical Engineering*, 2022, 41:482 [[Crossref](#)], [[Google Scholar](#)], [[Publisher](#)]
- [9] Kubba R.M., Al-Joborry N.M., Theoretical study of a new oxazolidine-5-one derivative as a corrosion inhibitor for carbon steel surface, *Iraqi Journal of Science*, 2021, 1396 [[Crossref](#)], [[Google Scholar](#)], [[Publisher](#)]
- [10] Nyijime T., Chahul H., Ayuba A., Iorhuna F., Theoretical investigations on thiadiazole derivatives as corrosion inhibitors on mild steel, *Advanced Journal of Chemistry-Section A*, 2023, 6:141 [[Crossref](#)], [[Google Scholar](#)], [[Publisher](#)]
- [11] Al-Rudaini K.A.K., Al-Saadie K.A.S., Milk Thistle Leaves Aqueous Extract as a New Corrosion Inhibitor for Aluminum Alloys in Alkaline Medium, *Iraqi Journal of Science*, 2021, 363 [[Crossref](#)], [[Google Scholar](#)], [[Publisher](#)]
- [12] Mohammed M.A., Kubba R.M., Experimental Evaluation for the Inhibition of Carbon Steel Corrosion in Salt and Acid Media by New Derivative of Quinolin-2-One, *Iraqi Journal of Science*, 2020, 1861 [[Crossref](#)], [[Google Scholar](#)], [[Publisher](#)]
- [13] Mammeri S., Chafai N., Harkat H., Kerkour R., Chafaa S., Protection of steel against corrosion in acid medium using dihydropyrimidinone derivatives: experimental and DFT study, *Iranian Journal of Science and Technology, Transactions A: Science*, 2021, 45:1607 [[Crossref](#)], [[Google Scholar](#)], [[Publisher](#)]
- [14] Esan T., Oyeneyin O., Olanipekun A., Ipinloju N., Corrosion inhibitive potentials of some amino acid derivatives of 1, 4-naphthoquinone-DFT calculations, *Advanced Journal of Chemistry-Section A*, 2022, 5:263 [[Crossref](#)], [[Google Scholar](#)], [[Publisher](#)]
- [15] Kubba R.M., Al-Joborry, N.M., Al-Lami, N.J., Theoretical and experimental studies for

- inhibition potentials of imidazolidine 4-one and oxazolidine 5-one derivatives for the corrosion of carbon steel in Sea Water, *Iraqi Journal of Science*, 2020, 2776 [[Crossref](#)], [[Google Scholar](#)], [[Publisher](#)]
- [16] Yavari Z., Darijani, M., Dehdab, M., Comparative theoretical and experimental studies on corrosion inhibition of aluminum in acidic media by the antibiotics drugs, *Iranian Journal of Science and Technology, Transactions A: Science*, 2018, **42**:1957 [[Crossref](#)], [[Google Scholar](#)], [[Publisher](#)]
- [17] Al-Joborry N.M., Kubba R.M., Theoretical and Experimental Study for Corrosion Inhibition of Carbon Steel in Salty and Acidic Media by A New Derivative of Imidazolidine 4-One, *Iraqi Journal of Science*, 2020, 1842 [[Crossref](#)], [[Google Scholar](#)], [[Publisher](#)]
- [18] Belghiti M.E., Mihit M., Mahsoun A., Elmelouky A., Mghaiouini R., Barhoumi A., Dafali A., Bakasse M., El Mhammedi M.A., Abdennouri M., Studies of Inhibition effect "E & Z" Configurations of hydrazine Derivatives on Mild Steel Surface in phosphoric acid. *Journal of Materials Research and Technology*, 2019, **8**:6336 [[Crossref](#)], [[Google Scholar](#)], [[Publisher](#)]
- [19] Kadhim M.M., Juber L.A.A., Al-Janabi A.S., Estimation of the Efficiency of Corrosion Inhibition by Zn-Dithiocarbamate Complexes: a Theoretical Study, *Iraqi Journal of Science*, 2021, 3323 [[Crossref](#)], [[Google Scholar](#)], [[Publisher](#)]
- [20] Glossman-Mitnik D., Computational study of the chemical reactivity properties of the Rhodamine B molecule, *Procedia Computer Science*, 2013, **18**:816 [[Crossref](#)], [[Google Scholar](#)], [[Publisher](#)]
- [21] Nahlé A., Salim R., El Hajjaji F., Aouad M., Messali M., Ech-Chihbi E., Hammouti B., Taleb M., Novel triazole derivatives as ecological corrosion inhibitors for mild steel in 1.0 M HCl: experimental & theoretical approach, *RSC advances*, 2021, **11**:4147 [[Crossref](#)], [[Google Scholar](#)], [[Publisher](#)]
- [22] Eddy N.O., Ameh P.O., Essien N.B., Experimental and computational chemistry studies on the inhibition of aluminium and mild steel in 0.1 M HCl by 3-nitrobenzoic acid, *Journal of Taibah University for Science*, 2018, **12**:545 [[Crossref](#)], [[Google Scholar](#)], [[Publisher](#)]
- [23] Guo L., Zhu M., Chang J., Thomas R., Zhang R., Wang P., Zheng X., Lin Y., Marzouki R., Corrosion Inhibition of N80 Steel by Newly Synthesized Imidazoline Based Ionic Liquid in 15% HCl Medium: Experimental and Theoretical Investigations, *International Journal of Electrochemical Science*, 2021, **16**:211139 [[Crossref](#)], [[Google Scholar](#)], [[Publisher](#)]
- [24] Lgaz H., Masroor S., Chafiq M., Damej M., Brahmia A., Salghi R., Benmessaoud M., Ali I.H., Alghamdi M.M., Chaouiki A., Evaluation of 2-mercaptobenzimidazole derivatives as corrosion inhibitors for mild steel in hydrochloric acid, *Metals*, 2020, **10**:357 [[Crossref](#)], [[Google Scholar](#)], [[Publisher](#)]
- [25] Gibson J.K., Bond Dissociation Energies Reveal the Participation of d Electrons in f-Element Halide Bonding, *The Journal of Physical Chemistry A*, 2022, **126**:272 [[Crossref](#)], [[Google Scholar](#)], [[Publisher](#)]
- [26] Kılınççeker G., Baş M., Zarifi F., Sayın K., Experimental and Computational Investigation for (E)-2-hydroxy-5-(2-benzylidene) Aminobenzoic Acid Schiff Base as a Corrosion Inhibitor for Copper in Acidic Media, *Iranian Journal of Science and Technology, Transactions A: Science*, 2021, **45**:515 [[Crossref](#)], [[Google Scholar](#)], [[Publisher](#)]
- [27] Iorhuna F., Thomas N.A., Lawal S.M., A Theoretical properties of Thiazepine and its derivatives on inhibition of Aluminium Al (110) surface. *Algerian Journal of Engineering and Technology*, 2023, **8**:43 [[Google Scholar](#)], [[Publisher](#)]
- [28] Oyeneyin O., Obadawo B., Ojo F., Akerele D., Akintemi E., Ejelonu B., Ipinloju N., Experimental and theoretical study on the corrosion inhibitive potentials of schiff base of aniline and

salicylaldehyde on mild steel in 0.5 M HCl, *Advanced Journal of Chemistry-Section B*, 2020, **2020**:197 [[Crossref](#)], [[Google Scholar](#)], [[Publisher](#)]

[29] Shehu U., Usman B., Corrosion Inhibition of Iron Using Silicate Base Molecules: A Computational Study, *Advanced Journal of*

*Chemistry, Section A*, 2023, **6**:334 [[Crossref](#)], [[Publisher](#)]

[30] Al-Amiery A.A., Mohamad A.B., Kadhum A.A.H. Experimental and theoretical study on the corrosion inhibition of mild steel by nonanedioic acid derivative in hydrochloric acid solution. *Sci Rep* 2022, **12**:4705 [[Crossref](#)], [[Google Scholar](#)], [[Publisher](#)]